The Long Noncoding RNA H19 Promotes Fibrotic Processes in Lens Epithelial Cells

Hanrong Li, Liyang Ji, Haoyue Shen, Zhuo Guo, Yu Qin, Li Feng, and Jiangyue Zhao

Department of Ophthalmology, Fourth Affiliated Hospital of China Medical University, Shenyang, Liaoning Province, China

Correspondence: Jiangyue Zhao and Li Feng, Department of Ophthalmology, Fourth Affiliated Hospital of China Medical University, Shenyang, Liaoning Province 110033, China; jyzhao@cmu.edu.cn and lfeng@cmu.edu.cn.

Received: September 8, 2022
Accepted: May 22, 2023
Published: June 13, 2023

Citation: Li H, Ji L, Shen H, et al. The long noncoding RNA H19 promotes fibrotic processes in lens epithelial cells. *Invest Ophthalmol Vis Sci.* 2023;64(7):21. https://doi.org/10.1167/iovs.64.7.21

Purpose. The purpose of this study was to investigate the role of lncRNA H19 in epithelial-mesenchymal transition (EMT) and its molecular mechanism in fibrotic cataracts.

Methods. TGF-β2-induced EMT was induced in human lens epithelial cell line (HLECs) and rat lens explants to mimic posterior capsular opacification (PCO) in vitro and in vivo. Anterior subcapsular cataract (ASC) was induced in C57BL/6J mice. The long noncoding RNA (lncRNA) H19 (H19) expression was detected by RT-qPCR. Whole-mount staining of lens anterior capsule was used to detect α-SMA and vimentin. Lentiviruses carrying shRNA or H19 vector were transfected in HLECs to knockdown or overexpress H19. Cell migration and proliferation were characterized by EdU, Transwell, and scratch assay. EMT level was detected by Western blotting and immunofluorescence. The rAAV2 carrying mouse H19 shRNA was injected into ASC model mouse anterior chambers as a gene therapy to determine its therapeutic potential.

Results. PCO and ASC models were built successfully. We found H19 upregulation in PCO and ASC models in vivo and in vitro. Overexpression of H19 by lentivirus transfection increased cell migration, proliferation, and EMT. In addition, H19 knockdown by lentivirus suppressed cell migration, proliferation, and EMT levels in HLECs. Moreover, transfection of rAAV2 H19 shRNA alleviated fibrotic area in ASC mouse lens anterior capsules.

Conclusions. Excessive H19 participates in lens fibrosis. Overexpression of H19 increases, whereas knockdown of H19 ameliorates HLECs migration, proliferation, and EMT. These results demonstrate H19 might be a potential target for fibrotic cataracts.

Keywords: cataract, long noncoding RNA (lncRNA) H19, fibrosis, gene therapy

Fibrosis is a pathological process that can affect multiple organs and is involved in many fatal diseases. Severe fibrosis in essential organs, such as the liver and pulmonary system, results in a lower survival rate than that of cancer.[1,2] Abnormal epithelial–mesenchymal transition (EMT) initiated by cytokines is the core process of tissue fibrosis.[3] During this process, intercellular junctions become looser with excessive extracellular matrix secretion. Epithelial cells also acquire stronger migration and proliferation abilities.[3] Although fibrotic diseases can be lethal, the underlying mechanisms are unclear, and effective therapies are still needed. The lens has been regarded as an ideal experimental model to study the processes that give rise to fibrosis due to its avascular environment and relatively simple composition.[4–6] Posterior capsular opacification (PCO) and anterior subcapsular cataract (ASC) are two kinds of lens fibrotic diseases caused by lens epithelial fibrosis that result in impaired visual quality.[7] Therefore, further study of lens fibrosis is needed not only because the lens is an ideal model for fibrosis research but also because lens epithelial fibrosis is a pathogenic factor in disease.

PCO and ASC are two different types of cataracts that share similar molecular and cellular mechanisms. ASC is a kind of primary lens opacification that is mainly caused by trauma or cytokine irritation and is characterized by fibrotic plaques underneath the anterior subcapsule of the lens.[5] Recently, researchers have shown that ASC occurs as a complication of implantable collamer lens (ICL) surgery.[8] PCO, also known as secondary cataract, is a common long-term complication of cataract surgery. In PCO, fibrotic plaques form in front of the posterior lens capsule.[9] In patients under 40 years of age, the PCO incidence after cataract surgery can reach 70% to 78%.[10] In children, the incidence has been reported to be as high as 100%.[11] In ASC and PCO, intraocular upregulation of transforming growth factor-β (TGF-β) has long been recognized as the major initiator that induces lens epithelial cells to undergo the EMT process, in which they migrate to the acellular posterior capsule or form fibrotic plaques.[9] Therefore, inhibition of lens epithelial cell migration and proliferation by EMT regulation might be an effective therapy for treating or preventing ASC or PCO.

Long noncoding RNAs (lncRNAs) are a series of transcripts with more than 200 nucleotides that cannot be translated into proteins.[12] Extensive evidence has demonstrated that lncRNAs play a crucial role in organ fibrosis.[13,14] To date, only a few lncRNAs have been studied in PCO or ASC.[15,16] The lncRNA H19 is encoded by a highly conserved imprinted

gene located on chromosome 11p15.5.[17] Studies have shown that hepatocellular carcinoma (HCC) bone metastasis could be increased by H19 overexpression.[18] In breast cancer, H19 was shown to promote tamoxifen resistance by regulating autophagy levels.[19] However, the role of H19 in lens fibrosis is still unclear.

In the present study, we found that the lncRNA H19 was significantly upregulated in ASC and PCO in in vivo, semi-in vivo, and in vitro models. Upregulation of H19 is an inducing factor of lens epithelial cell fibrosis. In a human lens epithelial cell (HLEC) EMT model, knockdown of H19 suppressed proliferation, migration, and EMT in a transforming growth factor-β2-induced in vitro model. Moreover, short hairpin (sh)RNA treatment targeting H19 mediated by rAAV2 in an ASC mouse model reduced fibrotic progression of lens epithelial cells, providing a potential therapeutic target for fibrotic cataracts.

Methods and Materials

Cell Culture

The HLEC line HLE-B3 was kindly gifted by Dr. Qinyu. The cells were cultured in Dulbecco's modified Eagle's medium (DMEM; Gibco; Thermo Fisher Scientific, Inc.) containing 10% fetal bovine serum (FBS; Gibco; Thermo Fisher Scientific, Inc.) and 300 mg/L L-glutamine. The cells were cultured in a 37°C humidified incubator with 5% CO_2.

ASC Mouse Model

All animal experiments were approved by the Animal Ethics Committee of China Medical University. The ASC mouse model was established as described previously.[20] Briefly, before the model was established, 5-week-old C57BL/6J mice were anesthetized with pentobarbital sodium (70 mg/kg), and mydriasis was induced with tropicamide eye drops. In the center of the anterior capsule, a small incision was made through the right cornea by a 28-gauge hypodermic needle. The incision depth was approximately 300 µm. After 3.5 days and 7 days of healing (n = 30 in each group), the anterior lens capsules were harvested for RT–qPCR experiments. To interfere with H19 levels in lens epithelial cells, ASC model mice received 1 µL of rAAV ($1X10^{12}$) carrying GFP sequence and mouse H19 shRNA or negative control virus in the anterior chambers (Brain-VTA). After ASC injuries were created, rAAVs were immediately injected into the anterior chambers with a microsyringe (32-gauge, Hamilton). Thirty days later, the lenses were harvested for RT–qPCR (n = 30 mice per group) and whole-mount staining (n = 6 mice per group).

Rat Lens Explant EMT Model

Lenses from Wistar rats aged between 20 and 22 days were carefully removed and incubated with the anterior side up. Lenses were cultured in serum-free M199 medium (Gibco; Thermo Fisher Scientific, Inc.) and 0.1 mg/mL L-glutamine. The lenses were treated with 10 ng/mL TGF-β2 (PeproTech, Inc.) and the same volume of 0.1% BSA as a control. Three days and 7 days later (n = 15 in each group), anterior lens capsules were harvested for RT–qPCR.

Construction of a Stably Transfected Cell Line

Lentiviruses carrying shRNA or overexpressing the H19 vector were purchased from Shanghai GeneChem. HLE-B3 cells were incubated in 6-well plates at 70% to 80% confluence. Then, the culture medium was replaced by diluted virus in DMEM (MOI = 10). After 8 hours of transfection, the dilution was replaced with normal culture medium. Cells with stable H19 overexpression or downregulation were selected with 4 µg/mL puromycin for 1 week in a 37°C humidified incubator with 5% CO_2.

Cell Counting Kit-8 Assay

Cell proliferation assays were performed using a Cell Counting Kit-8 assay (CCK8; Beyotime Biotechnology, China) according to the manufacturer's instructions. A total of 2×10^4 cells were seeded and incubated in 96-well plates. After cellular attachment, the cells were treated with 1 ng/mL or 10 ng/mL TGF-β2. The control group was treated with the same volume of 0.1% BSA. Seventy-two hours later, 10 µL of CCK-8 solution was added to each well. The plate was incubated in a 37°C incubator for 2 hours before the absorbance at 450 nm was read by micrometer measurement.

Whole-Mount Staining for the Lens Anterior Capsule

The mice with ASC were euthanized, and the lenses were dissected under a light microscope (Olympus, Inc.). After fixation in 4% paraformaldehyde for 30 minutes at room temperature, the anterior capsule was isolated and blocked in 5% BSA for 1 hour at room temperature and permeated in 0.3% Triton X-100 for 1 hour at room temperature. After that, the capsules were incubated in primary antibodies against α-smooth muscle actin (α-SMA; 1:200; Abcam; cat. no. ab124964) and vimentin (1:200; Abcam; cat. no. ab92547) for 10 hours at 4°C. Next, lens capsules were incubated in 1:200-diluted goat anti-rabbit IgG (H+L) highly cross-adsorbed secondary antibody, Alexa Fluor 488 (cat. no. A-11034; Thermo Fisher Scientific, Inc.) for 1 hour at room temperature. After nuclear staining with DAPI (Thermo Fisher Scientific, Inc.) at a concentration of 300 nM for 5 minutes at room temperature, the anterior capsules of the lens were mounted on a microscope slide and observed and imaged by an Olympus fluorescence microscope system.

Immunofluorescence Staining of Cultured Cells

Cells were cultured on slides for 48 hours with or without TGF-β2 before fixation with 4% paraformaldehyde for 20 minutes. Subsequently, the cells were permeabilized with 0.5% Triton X-100 solution for 10 minutes and blocked with 5% BSA for 30 minutes at room temperature. After that, the cell slides were incubated with primary antibodies against vimentin (1:200; cat. no. ab92547; Abcam), α-SMA (1:200; cat. no. ab124964; Abcam), E-cadherin (1:200; cat. no. ab40772; Abcam), N-cadherin (1:200; cat. no. ab18203; Abcam), fibronectin (1:200; cat. no. ab268020; Abcam), and Col-I (1:200; cat. no. ab34710; Abcam) for over 10 hours at 4°C. The following day, the cell slides were incubated with 1:200-diluted goat anti-rabbit IgG (H+L) highly cross-adsorbed secondary antibody, Alexa Fluor 488 (cat. no. A-11034; Thermo Fisher Scientific, Inc.) for 1 hour at room temperature. Finally, nuclei were stained with DAPI (Thermo

Investigative Ophthalmology & Visual Science

Fisher Scientific, Inc.) at a concentration of 300 nM for 5 minutes at room temperature. The slides were observed and imaged by fluorescence microscopy.

EdU Assay

An EdU staining assay was used to evaluate cell proliferation after the stably transfected cells were treated with or without TGF-β2. Forty-eight hours after 2X10^4 HLE-B3 cells were seeded into 96-well plates, the cells were labeled with EdU (RiboBio, China; 100 µL/well) for 2 hours. Then, the cells were fixed with 4% paraformaldehyde for 30 minutes at room temperature. After that, 0.5% Triton X-100 solution was added and incubated for 10 minutes at room temperature. Later, the cells were incubated with 1X Apollo staining solution from the EdU kit (RiboBio, Inc.) for 30 minutes at room temperature. Finally, the cells were incubated with DAPI (Thermo Fisher Scientific, Inc.) at a concentration of 300 nM for 5 minutes at room temperature. The cells were counted and imaged by microscopy.

Cell Scratch Assay

Stably transfected HLE-B3 cells were seeded in 6-well plates. At a confluence of 100%, the cells were scratched with a sterile yellow plastic pipette tip (20 µL). Then, the cells were washed with PBS 3 times, and fresh non-FBS DMEM with or without TGF-β2 (10 ng/mL) was added. After incubation at 37°C and 5% CO_2 for 48 hours, the scratched areas were imaged and measured by ImageJ software (version 1.52; National Institutes of Health).

Transwell Assay

For the Transwell assay, stably transfected HLE-B3 cells were seeded in the upper Transwell chambers at a density of 1×10^5 cells per chamber. In the upper chambers, the cells were incubated with serum-free DMEM with or without 10 ng/mL TGF-β2. DMEM with 10% FBS was added to the lower chambers. After 24 hours of cell migration, the membranes were washed in PBS 3 times, fixed with 4% formaldehyde for 20 minutes at room temperature, and dyed with 0.1% crystal violet for 10 minutes. Finally, the membrane was cut and imaged. The cell number was counted by ImageJ (version 1.52; National Institutes of Health).

Real-Time Quantitative Polymerase Chain Reaction

Total RNA of the lens capsule or cells was isolated by RNAiso Plus (TaKaRa Bio, Inc.) according to the manufacturer's protocol. Genomic DNA was diminished, and cDNA was synthesized with the PrimeScript RT Master Mix kit (TaKaRa Bio, Inc.). The mRNA amount was quantitatively measured with a SYBR PrimeScript RT–qPCR kit (TaKaRa

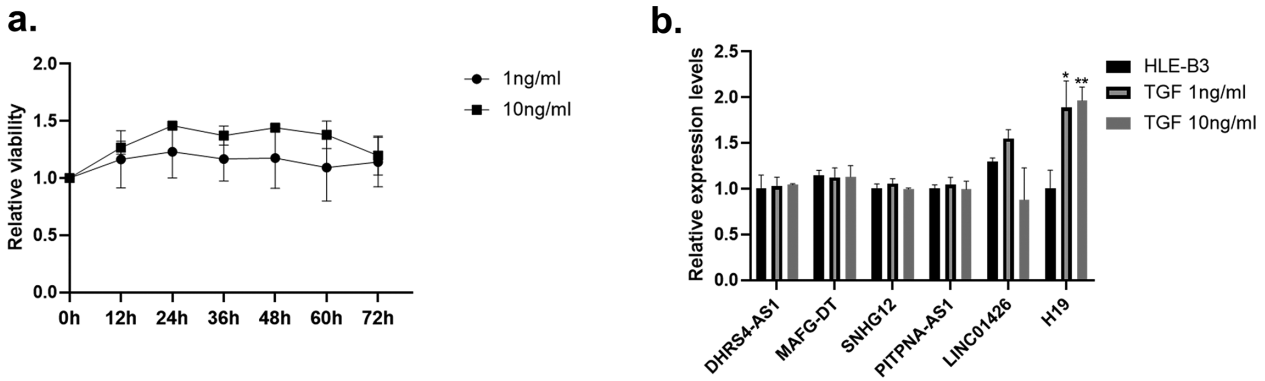

Figure 1. The lncRNA H19 is upregulated in the HLEC EMT model. (**a**) CCK8 assay showing that TGF-β2 promotes HLEC proliferation. (**b**) RT–qPCR analysis of H19 expression with or without TGF-β2 (1 ng/mL or 10 ng/mL) for 48 hours (*: $P < 0.05$, **: $P < 0.01$).

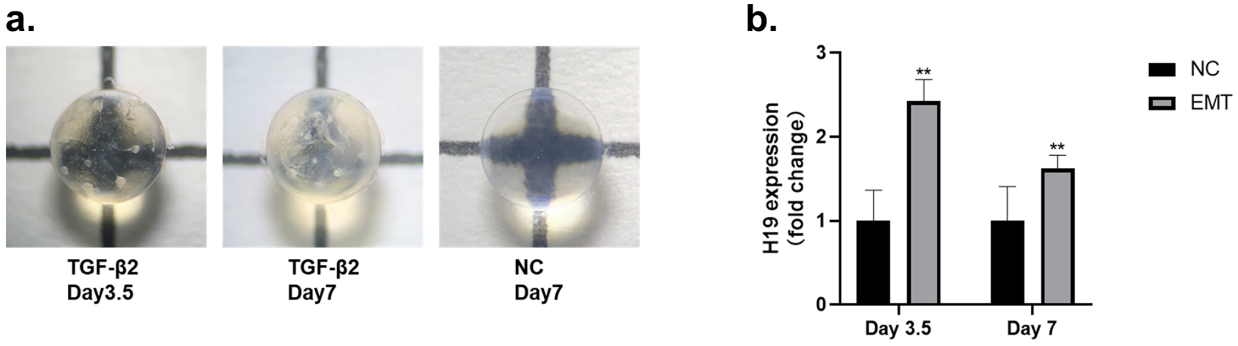

Figure 2. H19 is overexpressed in TGF-β2-treated rat lens explants. (**a**) Rat lens explants treated with TGF-β2 (10 ng/mL) for 3.5 and 7 days, and 7 days treated NC lens. Obvious capsular pearls and fibrosis occurred in the anterior capsule, and fibrous plaque were well formed after 7 days of treatment. (**b**) RT–qPCR analysis of H19 expression in TGF-β2-treated explants compared with normal explants (**: $P < 0.01$).

Investigative Ophthalmology & Visual Science

Bio, Inc.). The RT–qPCR experiments were performed by Roche 96. The relative expression level was obtained using the $2^{-\Delta\Delta Cq}$ method.[21] Glyceraldehyde 3-phosphate dehydrogenase (GAPDH) served as the internal control.

Western Blot

For cellular protein extraction, HLE-B3 cells per well were lysed in 100 µL of radioimmunoprecipitation assay (RIPA; Solarbio, Inc.) with protease inhibitor cocktail. After centrifugation at 12,000 × g for 30 minutes, the supernatants were mixed with 5X protein loading buffer. The samples were heated at 95°C for 15 minutes. Each sample was loaded onto an SDS–PAGE gel. After transfer to polyvinylidene difluoride (PVDF) membranes, the samples were incubated in targeted primary antibodies diluted 1:1000 at 4°C overnight. The primary antibodies were against GAPDH (cat. no. ab181602; Abcam), vimentin (cat. no. ab92547; Abcam), E-cadherin (cat. no. ab40772; Abcam), N-cadherin (cat. no. ab18203; Abcam), fibronectin (cat. no. ab268020; Abcam), and Col-I (cat. no. ab34710; Abcam). The next day, the membranes were incubated in horseradish peroxidase HRP-conjugated goat anti-rabbit IgG secondary antibodies (1:5,000; cat. no. ab6721; Abcam) for 1 hour at room temperature. Protein expression levels on the membrane were detected by Chemistar High-sig ECL Western blotting substrate (cat. no. 180-5001; Tanon Science and Technology Co., Ltd.). The expression levels were quantified using ImageJ (version 1.52; National Institutes of Health).

Statistical Analysis

All results presented in the figures are representative of three or more repeated experiments. All data are presented as the mean ± standard deviation (SD). GraphPad Prism 8.0 (GraphPad Software, USA) was used to perform the statistical analysis. Differences between the two groups were tested by independent samples *t* tests. Differences among multiple groups were tested using 1-way analysis of variance (ANOVA) and Tukey's post hoc test. A P value < 0.05 was considered statistically significant ($^{*}P < 0.05$, $^{**}P < 0.01$, and $^{***}P < 0.001$).

Results

H19 was Elevated in the TGF-β2-Induced EMT Model

TGF-β2, as a major isoform in the aqueous humor, plays essential regulatory roles in the eye.[22,23] We induced HLEB-3 EMT by TGF-β2 treatment. To determine a representative concentration and duration for TGF-β2-induced proliferation in an in vitro model, we examined HLE-B3 cell viability by CCK-8 assays (Fig. 1a). We found that cell viability was already improved by TGF-β2 in the first 12 hours and finally peaked at 48 hours, which was 1.44 times that at 0 hours with 10 ng/mL TGF-β2 treatment and 1.17 times that at 0 hours with 1 ng/mL TGF-β2 treatment. Treatment with 10 ng/mL TGF-β2 resulted in higher cell viability than 1 ng/mL treatment for 72 hours.

Thus, 48 hours was chosen as the experimental duration. The relative expression levels of 6 lncRNAs associated with EMT in other diseases, including the lncRNAs DHRS4-AS1,[24] MAFG-DT,[25] SNHG12,[26] PITPNA-AS1,[27] LINC01426,[28] and H19,[29] were assessed by RT–qPCR in the HLE-B3 cell EMT model. Only the expression of H19 showed significance in the experimental group compared to the control group. In both the 1 ng/mL and 10 ng/mL TGF-β2-treated groups,

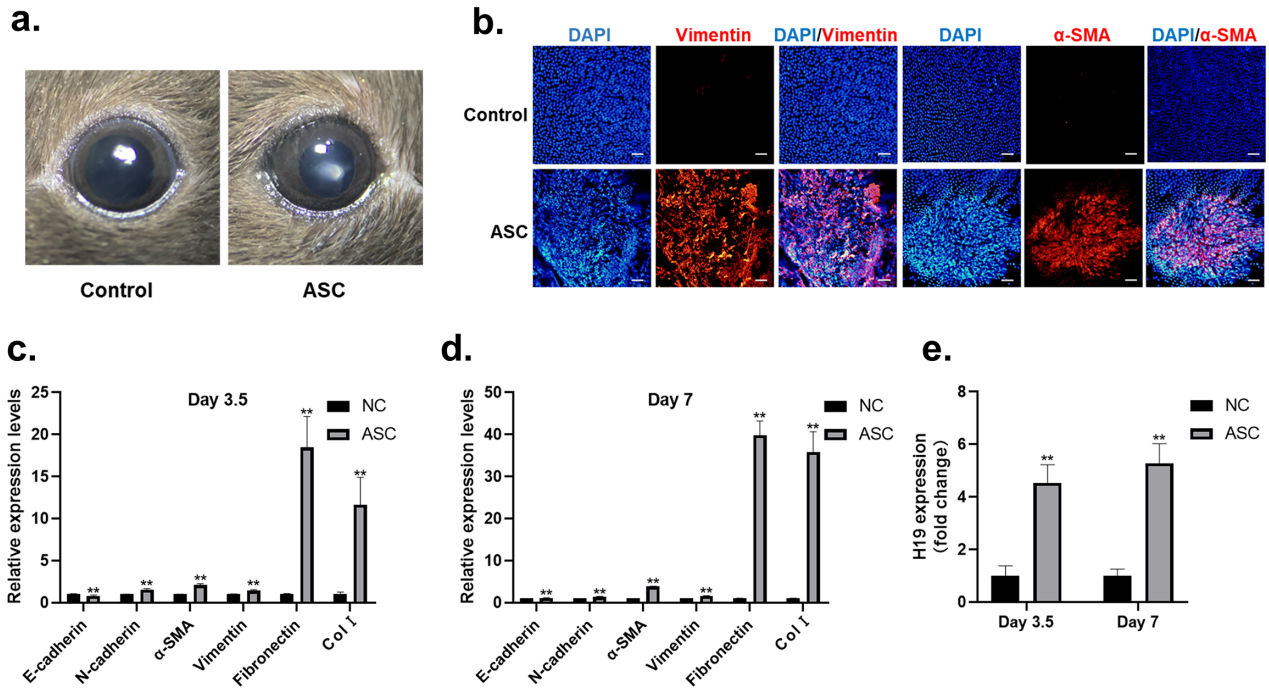

Figure 3. Overexpression of H19 in an in vivo ASC mouse model. (**a**) Pictures of ASC eyes. (**b**) Whole-mount staining of ASC lens capsules compared to the controls. *Red*: Targeted protein. *Blue*: DAPI. Scale bar = 100 µm. (**c, d**) Changes in EMT-related markers in the 3.5-day and 7-day ASC model lens capsules ($n = 3$). (**e**) RT–qPCR analysis of H19 expression levels in 3.5-day and 7-day lens epithelial cells compared to their self controls (**: $P < 0.01$).

Investigative Ophthalmology & Visual Science

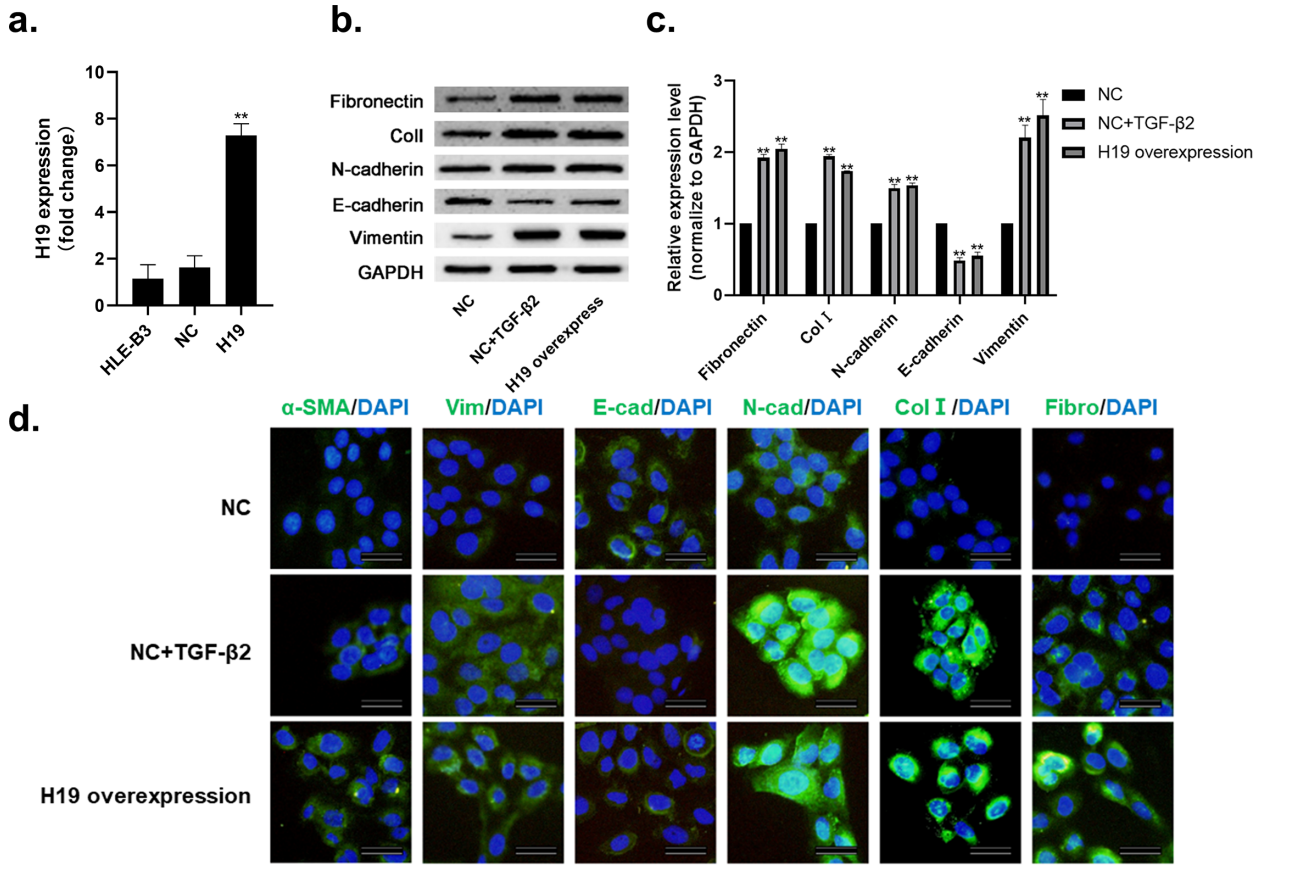

Figure 4. H19 induced EMT in HLECs. (**a**) RT–qPCR analysis of H19 expression levels in HLECs stably infected with plasmid virus and negative control virus. (**b, c**) Western blot analysis of EMT-related marker protein levels in the stable H19-overexpressing cell line and negative control virus-transfected cells ($n = 3$). (**d**) Immunofluorescence staining images of EMT-related markers in the stable H19-overexpressing cell line and negative control virus-transfected cells. *Green*: Target protein staining. Blue: DAPI staining. Scale bar = 50 µm. TGF-β2 treatment: 10 ng/mL, 48 hours (**: $P < 0.01$).

H19 was upregulated by approximately 2 times compared with that of the control group, as determined by RT–qPCR (Fig. 1b).

Upregulation of H19 in the Lens Capsule of EMT Rat Lens Explants

According to the reference, we constructed the rat lens explant EMT model. As shown in Figure 2a, after 3.5 days of 10 ng/mL TGF-β2 treatment, obvious capsular pearls and fibrosis occurred in the anterior capsule, and fibrous plaque were well formed after 7 days of treatment. RT–qPCR results demonstrated that H19 was augmented on both 3.5 days (2.5 times, $P < 0.001$) and 7 days (2 times, $P < 0.01$) compared to that of the control group (Fig. 2b).

Expression of H19 is Upregulated in the Lens Capsule of the ASC Mouse Model

To further demonstrate H19 regulation in the fibrous lens anterior capsule in vivo, we detected H19 expression in an injury-induced mouse ASC model. At 7 days, the lens developed obvious plaques underneath the anterior capsule of the lens in the middle of the lens (Fig. 3a). Obvious α-SMA and vimentin overexpression was found in anterior plaques of experimental lenses by whole-mount immunofluorescence staining of the lens anterior capsule, which suggested EMT-derived fibrotic lesion formation (Fig. 3b). Next, RNA was extracted from ASC model mouse anterior capsules and negative control (NC) mouse anterior capsules and analyzed by RT–qPCR. On certain days after injury, EMT was augmented compared to that in the uninjured eye (Figs. 3c, 3d). Transcriptional levels of N-cadherin (1.54 times on day 3.5 and 1.36 times on day 7), α-SMA (2.11 times on day 3.5 and 3.83 times on day 7), vimentin (1.43 times on day 3.5 and 1.6 times on day 7), fibronectin (18 times on day 3.5 and 39 times on day 7), and COL I (11 times on day 3.5 and 36 times on day 7) were upregulated, and E-cadherin was downregulated in the ASC mouse group (0.83 times on day 3.5). The mRNA level of H19 was also tested by RT–qPCR. The results showed that in the ASC group, the expression of H19 was significantly improved at both 3.5 days (4.5 times higher than that in the NC group) and 7 days (6 times higher than that in the NC group) after injury (Fig. 3e). H19 upregulation demonstrated a positive correlation with EMT levels in the ASC mouse model. We clearly observed significant upregulation of H19 in all 3 models, these results indicated that H19 might play an important role in the pathology of the lens epithelial cell fibrotic process.

Investigative Ophthalmology & Visual Science

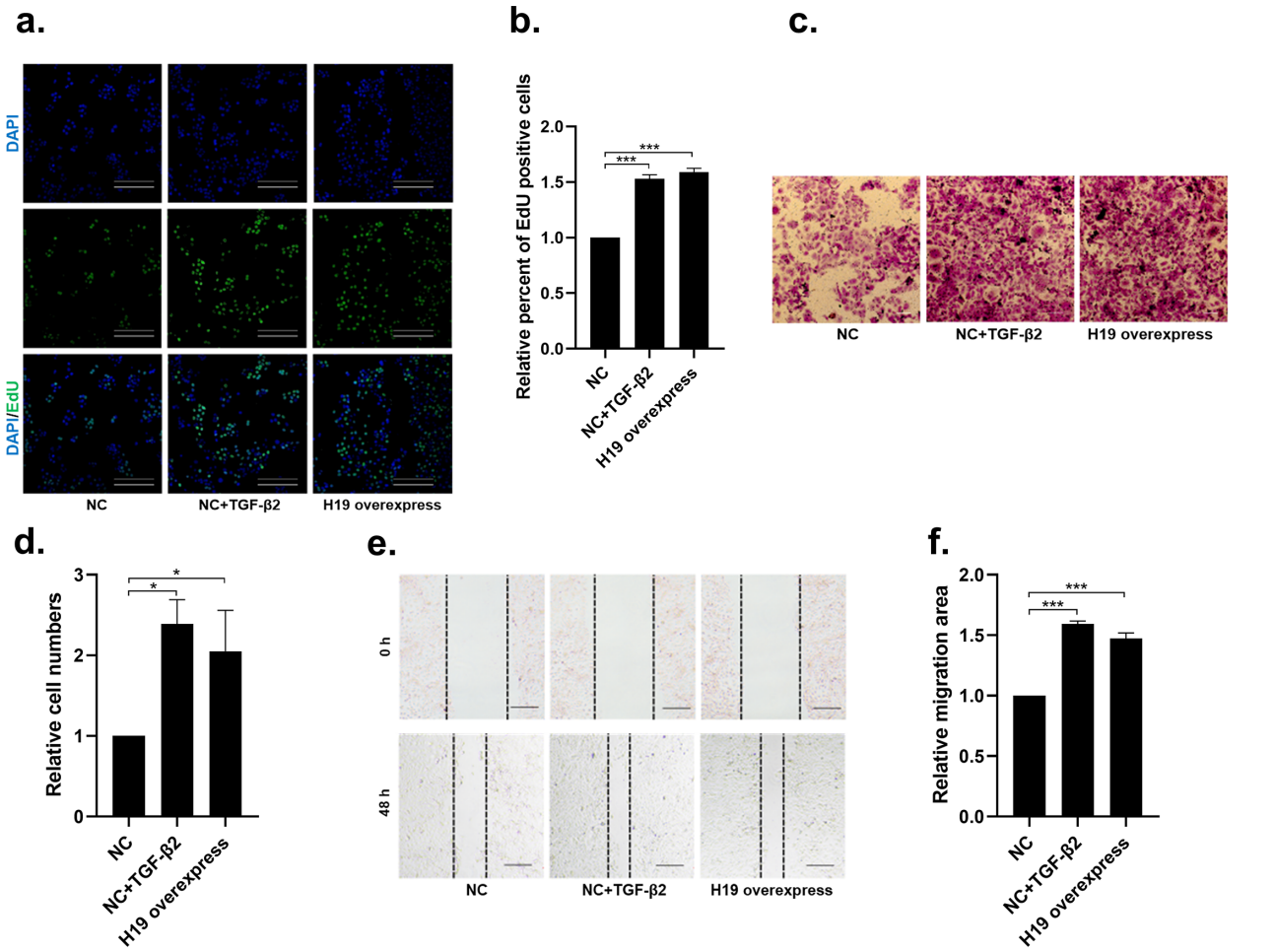

Figure 5. The lncRNA H19 promotes HLEC migration and proliferation. (**a, b**) EdU staining experiments and quantification showed that cell proliferation increased after upregulation of H19. *Green:* EdU staining. *Blue*: DAPI staining. Scale bar = 50 µm. (**c, d**) Transwell assays and quantification showed that H19 increased the number of migrated cells. Scale bar = 100 µm. (**e, f**) Scratch assay and quantity in the stable H19-upregulated HLEB-3 cell line, 10 ng/mL TGF-β2-treated stable H19-upregulated HLE-B3 cell line, and 10 ng/mL TGF-β2-treated negative control virus-transfected cells 48 hours after scratching. Scale bar = 100 µm. TGF-β2 treatment: 10 ng/mL, 48 hours (*: $P < 0.05$, ***: $P < 0.001$).

H19 Promoted Lens Epithelial Cell Migration and Proliferation

To demonstrate our hypothesis of the role of H19 in fibrotic cataracts, we transfected the HLE-B3 cell line with lentivirus carrying vectors overexpressing H19. The H19 expression in the transfected cell line was 7 times higher than that in the NC group, as shown by RT–qPCR (Fig. 4a), similar to that in the in vivo ASC model. An EdU staining assay was performed to detect the proliferation of HLE-B3 cells with or without stable H19 overexpression. We found that there was a significantly higher percentage of HLE-B3 cells in S phase after transfection with H19 pc-DNA (1.52 times) than after transfection with NC virus (Figs. 5a, 5b). We performed Transwell assays and wound healing experiments to detect the migration of HLE-B3 cells with or without H19 overexpression. The Transwell assay showed higher migration in the H19-overexpressing group than in the NC group, which was 2.5 times greater than that in the NC group (Figs. 5c, 5d). We also presented similar results by wound healing assays. In the wound healing experiment, the H19-overexpressing group showed a 1.5 times larger migration area than the NC group at 48 hours after scratching (Figs. 5e, 5f).

Elevated H19 Expression Induced Lens Epithelial Cell EMT

Compared to the NC cells, the H19-augmented HLE-B3 cells showed significantly higher expression of fibronectin, N-cadherin, COL I, and vimentin and lower levels of E-cadherin by Western blots (Figs. 4b, 4c). The same results were detected by immunofluorescence staining (Fig. 4d). The fluorescence intensity and area of EMT biomarkers in the H19 group were higher than those in the NC group. Collectively, H19 overexpression in HLECs initiated the HLEC-EMT process.

H19 Ablation Inhibited TGF-β2-Induced Lens Epithelial Cell Proliferation and Migration

To explore the functions of H19 in TGF-β2-induced HLEC-EMT, we transfected H19 shRNA into HLE-B3 cells with a knockdown efficiency of approximately 70% (Fig. 6a).

Investigative Ophthalmology & Visual Science

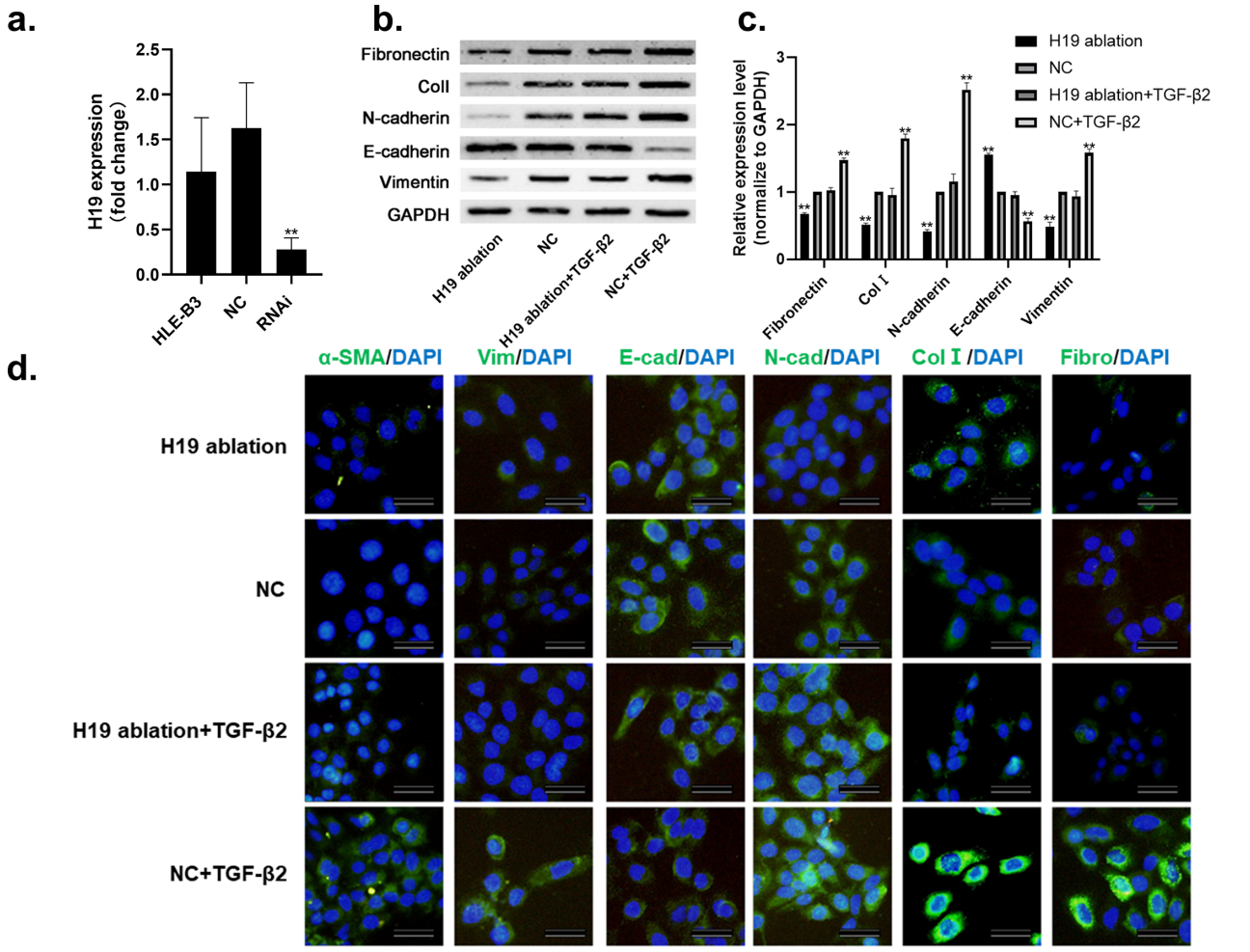

Figure 6. Downregulation of H19 inhibited TGF-β2-induced EMT in HLECs. (**a**) RT–qPCR analysis of H19 expression levels in HLECs stably transfected with shRNA virus and virus negative control. (**b, c**) Western blot analysis of EMT-related marker protein levels in TGF-β2-treated stable H19-downregulated cells and TGF-β2-treated negative control virus-transfected cells ($n = 3$). (**d**) Immunofluorescence staining images of EMT-related markers in TGF-β2-treated stable H19-downregulated cells and TGF-β2-treated negative control virus-transfected cells. *Green*: Target protein staining. Blue: DAPI staining. Scale bar = 50 µm. TGF-β2 treatment: 10 ng/mL, 48 hours (**: $P < 0.01$).

TGF-β2-induced EMT was further investigated in HLE-B3 cells as an in vitro model. Knockdown of H19 suppressed cell proliferation and abolished TGF-β2-induced proliferation in HLE-B3 cells (Figs. 7a, 7b). In the EdU assay, the proliferation ability of the H19 ablation group showed significant suppression compared to that of the NC group. In addition, compared to that in the TGF-β2-treated NC group, proliferation ability was downregulated in the TGF-β2-treated H19 ablation group. Furthermore, H19 knockdown markedly inhibited Transwell migration induced by TGF-β2 in HLE-B3 cells (Figs. 7c, 7d). Fewer cells that migrated to the bottom of the chamber (0.8 times that of the NC group) were found in the H19 knockdown group. Moreover, H19 knockdown suppressed the migration of HLE-B3 cells induced by TGF-β2. The wound healing experiment also achieved the same results (Figs. 7e, 7f).

H19 Mediated TGF-β2-Induced Lens Epithelial Cell EMT

Increased fibronectin, N-cadherin, COL I, and vimentin levels and decreased E-cadherin levels were shown by Western blotting and immunofluorescence staining in the TGF-β2-stimulated group (Figs. 6b, 6d). However, in the rescue experiment, H19 ablation reduced TGF-β2-induced EMT in the HLE-B3 cell line. We found that H19 ablation reduced fibronectin, N-cadherin, COL I, and vimentin and sustained E-cadherin protein expression in the TGF-β2-induced in vitro EMT group compared to the NC group (see Figs. 6b, 6c). Moreover, the same results were detected by immunofluorescence staining (see Fig. 6d). In short, H19 mediated the TGF-β2-induced HLEC-EMT process.

rAAV2-H19 shRNA Decreased the Fibrotic Area of the ASC Model Mouse Lens Anterior Capsules

The interference efficiency of mouse H19 shRNA was detected and verified by RT–qPCR (Fig. 8a). The rAAV2-H19 shRNA-transduced region was identified by the green fluorescent protein (GFP) signal before whole-mount staining (Fig. 8b). Vimentin expression revealed a smaller fibrotic area in the anterior capsule from the rAAV2-H19 shRNA group compared to the NC group by whole-mount staining (Fig. 8c). Statistical analysis showed a significant reduction in the fibrotic area in the rAAV2-H19 shRNA group compared to the NC group (Fig. 8d).

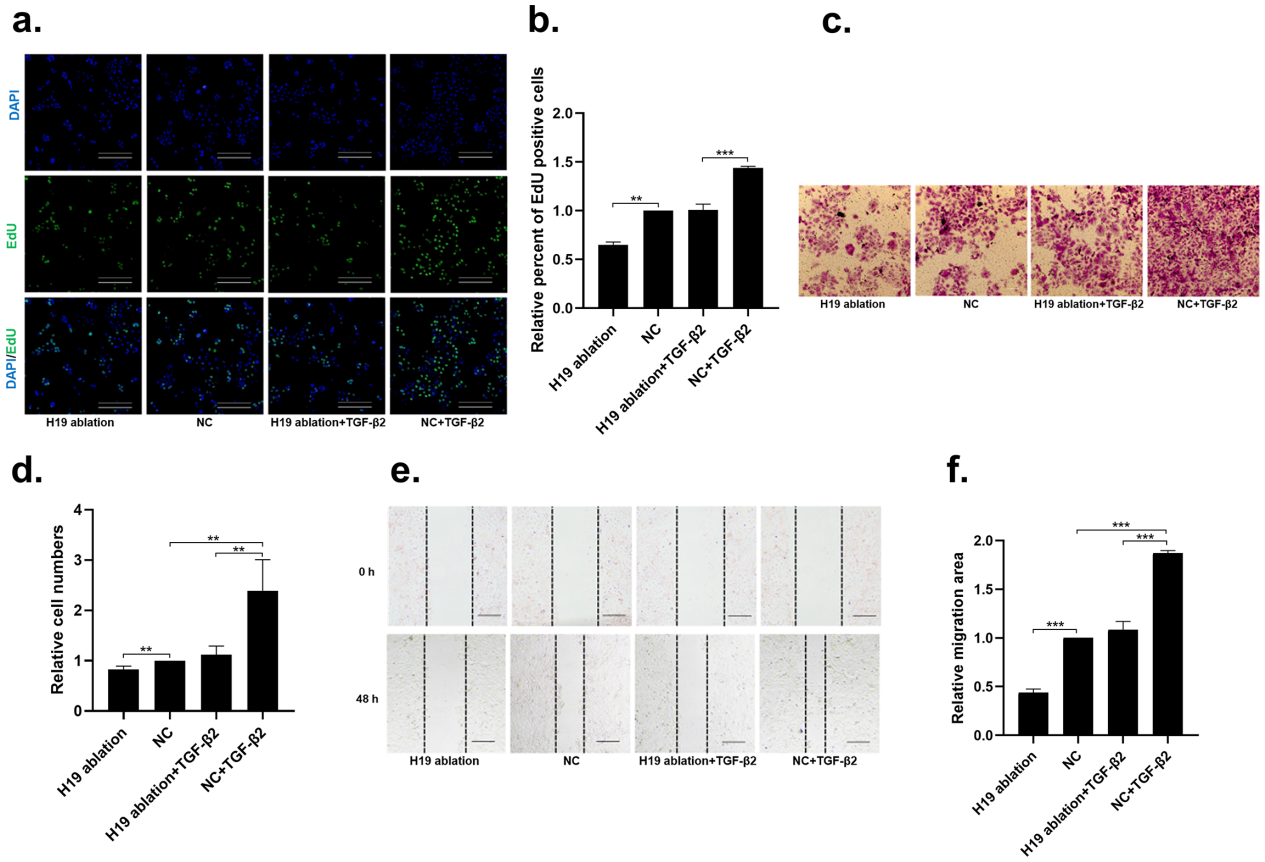

Figure 7. Knockdown of H19 can prevent TGF-β2-induced proliferation and migration of HLE-B3 cells. (**a, b**) EdU staining and quantification were used to detect cell proliferation. *Green:* EdU staining. Blue: DAPI staining. Scale bar = 50 µm. (**c, d**) Transwell assays and quantification showed that knockdown of H19 reduced the number of migrated cells. Scale bar = 100 µm. (**e, f**) Scratch assay and quantification of TGF-β2-treated negative control virus-transfected cells. The stable TGF-β2-treated H19-downregulated HLEC cells, stable H19-downregulated HLEC strain, and negative control virus-transfected cells 48 hours after scratching. Scale bar = 100 µm. TGF-β2 treatment: 10 ng/mL, 48 hours (**: $P < 0.01$, ***: $P < 0.001$).

Discussion

Lens anterior capsule fibrosis is considered a main pathological cause of ASC. Many studies on artificial intraocular lenses committing to reducing lens epithelial fibrosis have revealed the importance of fibrosis in the pathogenesis of ASC and PCO. TGF-β2 plays a major role in this process.[23,30] However, more potential factors involved in this pathological process need to be explored.

In the present study, we demonstrated a promoting role of H19 in the fibrotic process of lens epithelial cells. H19 was markedly overexpressed in mouse ASC models, rat lens explant EMT models and TGF-β2-induced in vitro models. Overexpression of H19 initiated and mediated the fibrotic process in HLECs. Knockdown of H19 in HLECs not only reduced mesenchymal features but also suppressed the TGF-β2-induced EMT process. Moreover, fibrotic areas were reduced after treatment with rAAV2-H19 shRNA in injury-induced ASC mouse lens anterior capsules, revealing the therapeutic potential of H19 in fibrotic cataracts.

Among the 6 lncRNAs we selected that have been demonstrated to regulate the EMT process in other diseases, only H19 was markedly upregulated in the TGF-β2-treated HLE-B3 cell line. To further verify the expression changes of H19 in fibrotic cataracts, we established a semi-in vivo EMT model and an in vivo ASC model. In the semi-in vivo model, rat lenses were explanted in M199 medium. TGF-β2 was added to the culture medium to imitate cytokine changes in the aqueous humor after cataract surgery. The expression level of H19 in the lens capsule was markedly increased after treatment for 3.5 days, which was higher than that at 7 days. This finding might be due to the promoting role of H19 occurring in the early step of EMT. Similar expression trends were also detected in renal fibrosis. In a report by Shi et al., H19 was overexpressed in 20-week-old CD-1 mice. However, the rate of increase was attenuated.[31] Similar results were also found in our ASC model. On day 3.5, H19 was highly upregulated in the injured lens capsule, and the upregulation rate slowed down in the next 3.5 days. The H19 gene is maternally imprinted and encodes the 2.3 kb H19 long noncoding RNA sharing the same locus with IGF2. Moreover, H19 is a precursor of miR-675.[32] The H19 has been reported to be involved in fibrotic processes in several organs, including cardiac fibrosis, kidney fibrosis, oral submucous fibrosis, pulmonary fibrosis, muscle fibrosis, and liver fibrosis.[31,33–38] As H19 is a highly conserved and multifunctional gene, our findings indicated that upregulation of H19 may play an important role in fibrotic diseases.

To test our hypothesis, we stably transfected HLEB-3 cell lines with lentivirus to improve H19 expression levels. The viability and migration of HLE-B3 cells were both improved after overexpression of H19. Augmentation of these two

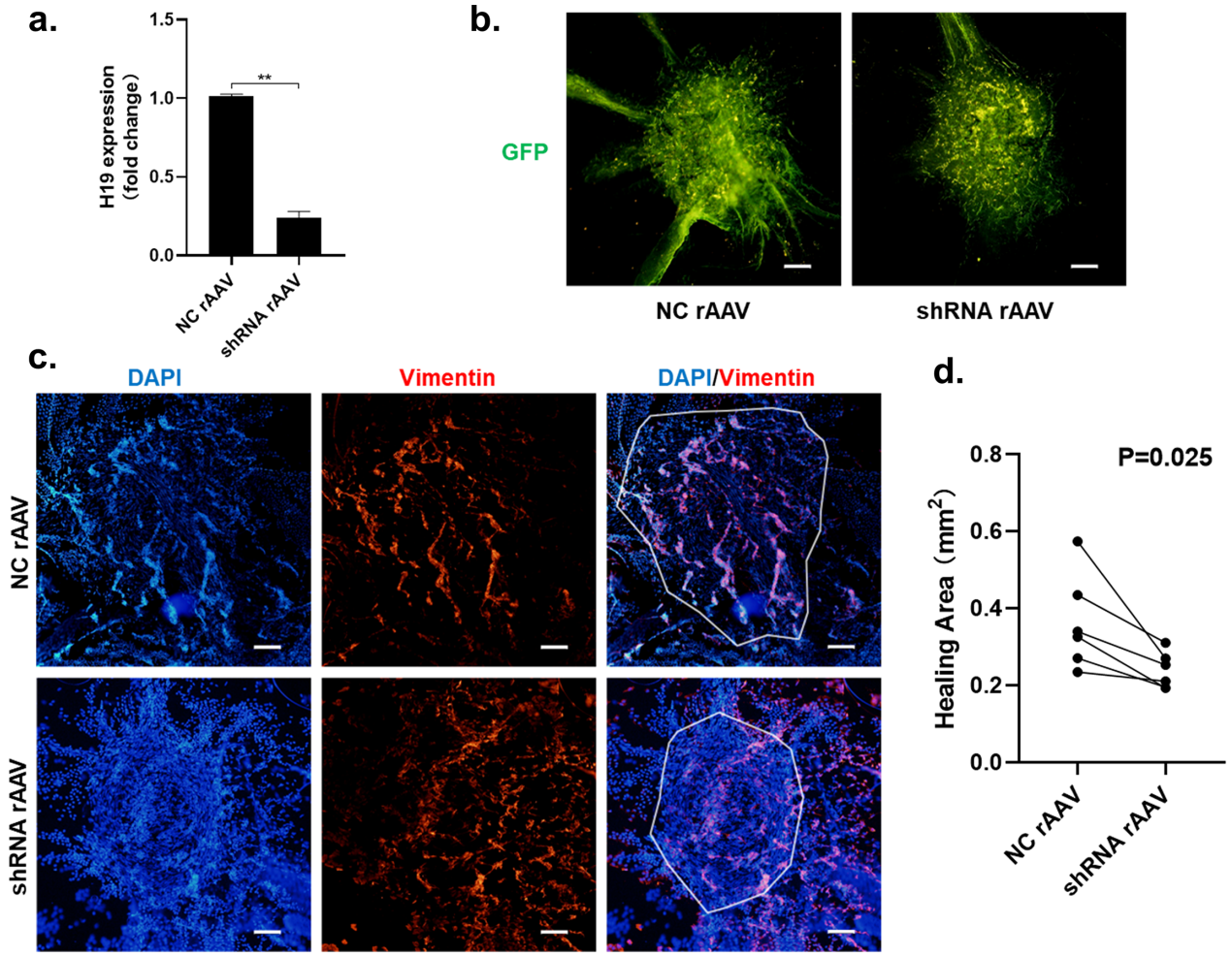

Figure 8. The rAAV2-H19 shRNA treatment reduced the lens capsule fibrotic area of mice with ASC. (**a**) RT–qPCR analysis of H19 expression changes after transfection with rAAV2- H19 shRNA. (**b**) Fluorescent images of GFP expression in rAAV2-transfected ASC lens capsules. Scale bar = 100 µm. (**c**) Immunofluorescence staining images of vimentin in rAAV2-treated ASC lens capsules. *Red*: Vimentin staining. Blue: DAPI staining. Scale bar = 100 µm. (**d**) Quantitative analysis of fibrotic area changes in ASC mouse lens capsules ($n = 6$).

characteristics made the lens epithelial cells remaining after cataract surgery more capable of migrating to the posterior capsule and proliferating to form fibrotic plaques or forming fibrotic plaques in the anterior capsule after lens injury.[39,40] There are three kinds of EMTs that contribute to embryogenesis, fibrosis, and cancer progression.[41] The pathological factor causing fibrotic cataracts is the second kind of EMT and is irreversible.[30] In the lens epithelial fibrotic process, the cells lose epithelial characteristics and gain mesenchymal characteristics, including excessive extracellular matrix, reduced cellular adhesion, and improved motility.[42] These proteins, which are regarded as EMT biomarkers, were detected in HLEB-3 cells. When H19 was upregulated, a higher EMT level was observed. Therefore, the findings supported the hypothesis that H19 could promote fibrosis in lens epithelial cells.

Next, we further explored whether ablation of H19 could inhibit fibrosis induced by TGF-β2 in lens epithelial cells. After being cultured with TGF-β2, the HLE-B3 cell line showed increased proliferation, migration, and EMT levels, which were successfully suppressed by stable knockdown of H19. These results indicated that H19 might have therapeutic potential in fibrotic cataracts. However, in vivo, factors other than TGF-β2, such as TNF-α, are involved in the induction of fibrosis in lens epithelial cells.[43] To further investigate the therapeutic effect of H19 on lens epithelial cell fibrosis in the presence of multiple cytokines, we performed rAAV2-H19 shRNA treatment in mice with ASC. The results showed significant suppression of fibrotic plaque formation by interference with H19 in the lens capsule. In ocular diseases, there are already drugs targeting RNA approved by the US Food and Drug Administration (FDA), and an increasing number of RNA-targeted drugs are being investigated in clinical trials.[44–46] The therapeutic effect of H19 interference in the ASC mouse model provides a novel strategy for the prevention and treatment of PCO and ASC. To induce fibrosis, H19 may function through some important pathways, including the canonical Smad pathway and noncanonical pathways. In kidney fibrosis in diabetic nephropathy and pulmonary fibrosis, H19 was verified to mediate EMT via the Smad3 pathway.[31,47] The variant of H19, which lacks exon 4, promotes oral cancer by binding ZEB1 mRNA.[48] By binding hnRNPA2B1, H19 promotes colorectal cancer metastasis.[49] Moreover, by directly antagonizing P53, the tumor suppressor H19 enhances breast cancer EMT.[50]

Investigative Ophthalmology & Visual Science

Interestingly, Lang et al.[51] reached the opposite conclusion about the functions of H19 in the lens epithelial cell fibrotic process. Instead of stable transfection, 24 hours of transient transfection of the H19 plasmid in HLECs inhibited EMT progression, revealing opposite roles of H19 in short-term upregulation versus long-term upregulation. Moreover, long-term treatment with H19 knockdown exhibited different efficacy than short-term treatment. After a month of H19 shRNA treatment in our study, the ASC mice showed shrunken fibrotic plaques of the anterior capsule. Stable transfection of H19 shRNA in HLECs exhibited EMT-inhibiting functions as well. However, in a study by Lang et al., short-term downregulation of H19 resulted in acceleration of EMT in HLECs. Shorter-term treatment, including the 24-hour upregulation of H19 in the fibrotic semi-in vivo mouse lens model and the 6-day upregulation of H19 in the fibrotic semi-in vivo human lens model in the study by Lang et al., led to inhibition of fibrotic plaque growth. A previous study has demonstrated that this may result from sponging of different microRNAs that play opposite roles in different stages of EMT progression.[29] Considering our research and Lang et al.'s research, treatment strategies targeting H19 in the earlier and later stages of lens epithelial cell fibrosis may have opposite effects, and it is better to upregulate H19 in the earlier stage and downregulate H19 in the later stage. Nevertheless, in the congenital H19 gene knockout mice in Lang et al.'s research, long-term knockout of H19 resulted in the phenotype of congenital cataract. Normal levels of H19 are essential for the normal growth and development of the lens. In addition, the application of different epithelial cell lines may have caused the conflicting results between our research and that of Lang et al.

In the field of tumor therapy, H19 has already been regarded as a novel therapeutic target.[52] Researchers consider H19 a biomarker in circulatory system disease.[53,54] However, the mechanisms underlying H19-induced HLEC fibrosis are still unclear. H19 may directly act on EMT-associated molecules instead of acting through signaling pathways. In oral submucous precancer fibrosis, H19 directly regulates one of the extracellular matrix components—COL1α.[33]

In conclusion, an in vitro EMT model was used to show for the first time that H19 is highly expressed and related to EMT marker protein expression in lens epithelial cells. The rat lens explant EMT model and the ASC mouse model were used to confirm the overexpression of H19 in the fibrotic process of lens epithelial cells. Importantly, H19 promotes the proliferation, migration, and EMT of lens epithelial cells in vitro. In the presence of TGF-β2, interference with H19 repressed cytokine-induced fibrosis. The inhibitory effect of H19 shRNA on fibrotic plaque formation was confirmed in the mouse ASC model, revealing a novel therapeutic strategy for fibrotic cataracts.

Acknowledgments

Supported by the National Natural Science Foundation of China to Z.J.Y. (No. 81870646 and No. 82070946).

Ethics Approval and Consent to Participate: Ethical approval of animal experiments was approved by the Ethics Committee of China Medical University (Shenyang, China).

Disclosure: **H. Li**, None; **L. Ji**, None; **H. Shen**, None; **Z. Guo**, None; **Y. Qin**, None; **L. Feng**, None; **J. Zhao**, None

References

1. Hung C, Linn G, Chow Y-H, et al. Role of lung pericytes and resident fibroblasts in the pathogenesis of pulmonary fibrosis. *Am J Respir Crit Care Med*. 2013;188(7):820–830.
2. Piersma B, Bank R. Collagen cross-linking mediated by lysyl hydroxylase 2: an enzymatic battlefield to combat fibrosis. *Essays Biochem*. 2019;63(3):377–387.
3. Su J, Morgani SM, David CJ, et al. TGF-β orchestrates fibrogenic and developmental EMTs via the RAS effector RREB1. *Nature*. 2020;577(7791):566–571.
4. Shirai K, Tanaka S-I, Lovicu FJ, Saika S. The murine lens: a model to investigate in vivo epithelial-mesenchymal transition. *Dev Dyn*. 2018;247(3):340–345.
5. Eldred J, Dawes L, Wormstone I. The lens as a model for fibrotic disease. *Philos Trans R Soc Lond B Biol Sci*. 2011;366(1568):1301–1319.
6. Walker J, Zhai N, Zhang L, et al. Unique precursors for the mesenchymal cells involved in injury response and fibrosis. *Proc Natl Acad Sci USA*. 2010;107(31):13730–13735.
7. Chen X, Xiao W, Chen W, et al. MicroRNA-26a and -26b inhibit lens fibrosis and cataract by negatively regulating Jagged-1/Notch signaling pathway. *Cell Death Differ*. 2017;24(8):1431–1442.
8. Lindland A, Heger H, Kugelberg M, Zetterström C. Vaulting of myopic and toric Implantable Collamer Lenses during accommodation measured with Visante optical coherence tomography. *Ophthalmology*. 2010;117(6):1245–1250.
9. Wederell E, de Iongh R. Extracellular matrix and integrin signaling in lens development and cataract. *Semin Cell Dev Biol*. 2006;17(6):759–776.
10. Morarescu D, West-Mays J, Sheardown H. Effect of delivery of MMP inhibitors from PDMS as a model IOL material on PCO markers. *Biomaterials*. 2010;31(8):2399–2407.
11. Hodge W. Posterior capsule opacification after cataract surgery. *Ophthalmology*. 1998;105(6):943–944.
12. McCabe E, Rasmussen T lncRNA involvement in cancer stem cell function and epithelial-mesenchymal transitions. *Semin Cancer Biol*. 2021;75:38–48.
13. Soni D, Biswas R. Role of non-coding RNAs in post-transcriptional regulation of lung diseases. *Front Genet*. 2021;12:767348.
14. He Y, Wang W, Jiang P, et al. Long non-coding RNAs in oral submucous fibrosis: their functional mechanisms and recent research progress. *J Inflamm Res*. 2021;14:5787–5800.
15. Ye W, Ma J, Wang F, et al. LncRNA MALAT 1 regulates miR-144-3p to facilitate epithelial-mesenchymal transition of lens epithelial cells via the ROS/NRF2/Notch1/Snail Pathway. *Oxid Med Cell Longev*. 2020;2020:8184314.
16. Yao L, Yang L, Song H, Liu T, Yan H. MicroRNA miR-29c-3p modulates FOS expression to repress EMT and cell proliferation while induces apoptosis in TGF-β2-treated lens epithelial cells regulated by lncRNA KCNQ1OT1. *Biomed Pharmacother*. 2020;129:110290.
17. Wang Y, Hylemon P, Zhou H. Long non-coding RNA H19: a key player in liver diseases. *Hepatology (Baltimore, Md.)*. 2021;74:1652–1659.
18. Huang Z, Chu L, Liang J, et al. H19 promotes HCC bone metastasis through reducing osteoprotegerin expression in a protein phosphatase 1 catalytic subunit alpha/p38 mitogen-activated protein kinase-dependent manner and sponging microRNA 200b-3p. *Hepatology. (Baltimore, Md.)*. 2020;74:214–232.
19. Wang J, Xie S, Yang J, et al. The long noncoding RNA H19 promotes tamoxifen resistance in breast cancer via autophagy. *J Hematol Oncol*. 2019;12(1):81.
20. Xiao W, Chen X, Li W, et al. Quantitative analysis of injury-induced anterior subcapsular cataract in the mouse:

a model of lens epithelial cells proliferation and epithelial-mesenchymal transition. *Sci Rep*. 2015;5:8362.
21. Livak KJ, Schmittgen TD. Analysis of relative gene expression data using real-time quantitative PCR and the 2−ΔΔCT method. *Methods*. 2001;25(4):402–408.
22. Lovicu FJ, Shin EH, McAvoy JW. Fibrosis in the lens. Sprouty regulation of TGFβ-signaling prevents lens EMT leading to cataract. *Exp Eye Res*. 2016;142:92–101.
23. Kubo E, Shibata T, Singh DP, Sasaki H. Roles of TGF β and FGF signals in the lens: tropomyosin regulation for posterior capsule opacity. *Int J Mol Sci*. 2018;19(10):3093.
24. Yan F, Zhao W, Xu X, et al. LncRNA DHRS4-AS1 inhibits the stemness of NSCLC cells by sponging miR-224-3p and upregulating TP53 and TET1. *Front Cell Dev Biol*. 2020;8:585251.
25. Jia YC, Wang JY, Liu YY, Li B, Guo H, Zang AM. LncRNA MAFG-AS1 facilitates the migration and invasion of NSCLC cell via sponging miR-339-5p from MMP15. *Cell Biol Int*. 2019;43(4):384–393.
26. Chen PP, Zhang Z-S, Wu J-C, Zheng J-F, Lin F. LncRNA SNHG12 promotes proliferation and epithelial mesenchymal transition in hepatocellular carcinoma through targeting HEG1 via miR-516a-5p. *Cell Signal*. 2021;84:109992.
27. Chen G, Zheng Z, Li J, et al. Long non–coding RNA PITPNA–AS1 silencing suppresses proliferation, metastasis and epithelial–mesenchymal transition in non–small cell lung cancer cells by targeting microRNA–32–5p. *Mol Med Rep*. 2021;23(3):212.
28. Liu X, Yin Z, Xu L, et al. Upregulation of LINC01426 promotes the progression and stemness in lung adenocarcinoma by enhancing the level of SHH protein to activate the hedgehog pathway. *Cell Death Dis*. 2021;12(2):173.
29. Zhou W, Ye X-L, Xu J, et al. The lncRNA H19 mediates breast cancer cell plasticity during EMT and MET plasticity by differentially sponging miR-200b/c and let-7b. *Sci Signal*. 2017;10(483):eaak9557.
30. Shu D, Lovicu F. Myofibroblast transdifferentiation: the dark force in ocular wound healing and fibrosis. *Prog Retin Eye Res*. 2017;60:44–65.
31. Shi S, Song L, Yu H, et al. Knockdown of LncRNA-H19 ameliorates kidney fibrosis in diabetic mice by suppressing miR-29a-mediated EndMT. *Front Pharmacol*. 2020;11:586895.
32. Venkatraman A, He XC, Thorvaldsen JL, et al. Maternal imprinting at the H19-Igf2 locus maintains adult haematopoietic stem cell quiescence. *Nature*. 2013; 500(7462):345–349.
33. Yu C, Liao Y-W, Hsieh P-L, Chang Y-C. Targeting lncRNA H19/miR-29b/COL1A1 axis impedes myofibroblast activities of precancerous oral submucous fibrosis. *Int J Mol Sci*. 2021;22(4):2216.
34. Choong O, Chen C-Y, Zhang J, et al. Hypoxia-induced H19/YB-1 cascade modulates cardiac remodeling after infarction. *Theranostics*. 2019;9(22):6550–6567.
35. Xiao Y, Liu R, Li X, et al. Long noncoding RNA H19 contributes to cholangiocyte proliferation and cholestatic liver fibrosis in biliary atresia. *Hepatology (Baltimore, Md.)*. 2019;70(5):1658–1673.
36. Morgoulis D, Berenstein P, Cazacu S, et al. sPIF promotes myoblast differentiation and utrophin expression while inhibiting fibrosis in Duchenne muscular dystrophy via the H19/miR-675/let-7 and miR-21 pathways. *Cell Death Dis*, 2019;10(2):82.
37. Lin J, Luo Z, Liu S, Chen Q, Liu S, Chen J. Long non-coding RNA H19 promotes myoblast fibrogenesis via regulating the miR-20a-5p-Tgfbr2 axis. *Clin Exp Pharmacol Physiol*. 2021;48(6):921–931.
38. Xiao T, Zou Z, Xu J, et al. LncRNA H19-mediated M2 polarization of macrophages promotes myofibroblast differentiation in pulmonary fibrosis induced by arsenic exposure. *Environ Pollut (Barking, Essex : 1987)*. 2021;268(Pt A):115810.
39. Maedel S, Evans JR, Harrer-Seely A, Findl O., Intraocular lens optic edge design for the prevention of posterior capsule opacification after cataract surgery. *Cochrane Database Syst Rev*. 2021;8:CD012516.
40. Wang X, Wang L, Sun Y, et al. MiR-22-3p inhibits fibrotic cataract through inactivation of HDAC6 and increase of α-tubulin acetylation. *Cell Prolif*. 2020;53(11):e12911.
41. Mamuya F, Duncan M. aV integrins and TGF-β-induced EMT: a circle of regulation. *J Cell Mol Med*. 2012;16(3):445–455.
42. Yang J, Antin P, Berx G, et al. Guidelines and definitions for research on epithelial-mesenchymal transition. *Nat Rev Mol Cell Biol*. 2020;21(6):341–352.
43. DeDreu J, Bowen CJ, Logan CM, et al. An immune response to the avascular lens following wounding of the cornea involves ciliary zonule fibrils. *FASEB J*. 2020;34(7):9316–9336.
44. Pañeda C. SYL040012, a siRNA for the treatment of glaucoma. *Acta Ophthalmologica*. 2013;91(s252):Abstract 4227.
45. Moreno-Montañés J, Bleau AM, Jimenez AI. Tivanisiran, a novel siRNA for the treatment of dry eye disease. *Expert Opin Investig Drugs*. 2018;27(4):421–426.
46. Migliorati J, Liu S, Liu A, et al. Absorption, distribution, metabolism, and excretion of US Food and Drug Administration-approved antisense oligonucleotide drugs. *Drug Metabol Dispos*. 2022;50:888–897.
47. Wang X, Cheng Z, Dai L, et al. Knockdown of long noncoding RNA H19 represses the progress of pulmonary fibrosis through the transforming growth factor β/Smad3 pathway by regulating microRNA 140. *Mol Cell Biol*. 2019;39(12):e00143–19.
48. Zhou W, Wang X, Fang B. A variant of H19 transcript regulates EMT and oral cancer progression. *Oral Dis*. 2022;28:116–124.
49. Zhang Y, Huang W, Yuan Y, et al., Long non-coding RNA H19 promotes colorectal cancer metastasis via binding to hnRNPA2B1. *J Exp Clin Cancer Res*. 2020;39(1):141.
50. Li Y, Ma H-Y, Hu X-W, et al. LncRNA H19 promotes triple-negative breast cancer cells invasion and metastasis through the p53/TNFAIP8 pathway. *Cancer Cell Int*. 2020;20: 200.
51. Xiong L, Sun Y, Huang J, et al. Long non-coding RNA H19 prevents lens fibrosis through maintaining lens epithelial cell phenotypes. *Cells*, 2022;11(16):2559.
52. Shermane Lim Y, Xiang X, Garg M, et al. The double-edged sword of H19 lncRNA: insights into cancer therapy. *Cancer Lett*. 2021;500:253–262.
53. Omura J, Habbout K, Shimauchi T, et al. Identification of long noncoding RNA H19 as a new biomarker and therapeutic target in right ventricular failure in pulmonary arterial hypertension. *Circulation*. 2020;142(15):1464–1484.
54. Pagiatakis C, Hall I, Condorelli G. Long non-coding RNA H19: a new avenue for RNA therapeutics in cardiac hypertrophy? *Eur Heart J*. 2020;41(36):3475–3476.

Investigative Ophthalmology & Visual Science